NUCL SCI TECH (2022) 33:43
https://doi.org/10.1007/s41365-022-01029-7

Neutronic study on the effect of first wall material thickness on tritium production and material damage in a fusion reactor

Hacı Mehmet Şahin[1] · Güven Tunç[2] · Alper Karakoç[3] · Melood Mohamad Omar[3]

Received: 16 December 2021 / Revised: 25 January 2022 / Accepted: 22 February 2022 / Published online: 19 April 2022

Abstract In this study, the effects of changing first wall materials and their thicknesses on a reactor were investigated to determine the displacement per atom (DPA) and gas production (helium and hydrogen) in the first wall, as well as the tritium breeding ratio (*TBR*) in the coolant and tritium breeding zones. Therefore, the modeling of the magnetic fusion reactor was determined based on the blanket parameters of the International Thermonuclear Experimental Reactor (ITER). Stainless steel (SS 316 LN-IG), Oxide Dispersion Strengthened Steel alloy (PM2000 ODS), and China low-activation martensitic steel (CLAM) were used as the first wall (FW) materials. Fluoride family molten salt materials (FLiBe, FLiNaBe, FLiPb) and lithium oxide (LiO_2) were considered the coolant and tritium production material in the blanket, respectively. Neutron transport calculations were performed using the well-known 3D code MCNP5 using the continuous-energy Monte Carlo method. The built-in continuous energy nuclear and atomic data libraries along with the Evaluated Nuclear Data file (ENDF) system (ENDF/B-V and ENDF/B-VI) were used. Additionally, the activity cross-section data library CLAW-IV was used to evaluate both the DPA values and gas production of the first wall (FW) materials. An interface computer program written in the FORTRAN 90 language to evaluate the MCNP5 outputs was developed for the fusion reactor blanket. The results indicated that the best TBR value was obtained for the use of the FLiPb coolant, whereas depending on the thickness, the first wall replacement period in terms of radiation damage to all materials was between 6 and 11 years.

Keywords ITER · First wall material · Material damage · Tritium breeding ratio · Fluorides family molten salt materials

1 Introduction

Research on fusion energy for electricity production has primarily focused on the concepts of magnetic and inertial fusion energy. In the last 70 years, the concept of magnetic fusion has gained importance in the field of electricity generation from fusion energy. El-Guebaly [1] stated that the magnetic fusion concept based on a toroidal configuration of Toroidalnaya Kamera and Magnitnaya Katushka/Toroidal Chamber and Magnetic Coil (TOKAMAK) devices, and the International Thermonuclear Experimental Reactor (ITER) is one of the most important pioneers of this concept [2].

Several vital elements makeup the successful design of magnetic fusion reactors. The first element is the self-sufficient fuel cycle for plant sustainability. To design a self-sustained D-T fueled fusion reactor, tritium must be produced at least as much as it is consumed [3]. The ratio of tritium production to its consumption is determined as the net tritium breeding ratio (*TBR*), and to ensure its self-sufficiency, the *TBR* must be greater than 1.05 ($TBR > 1.05$) [4]. This is because a fraction of the fuel is

✉ Hacı Mehmet Şahin
mehmetsahin@karabuk.edu.tr

[1] Department of Energy Systems Engineering, Technology Faculty, Karabuk University, Karabuk, Turkey

[2] Department of Energy Systems Engineering, Technology Faculty, Gazi University, Ankara, Turkey

[3] Department of Energy Systems Engineering, Institute of Graduate Programs, Karabuk University, Karabuk, Turkey

commonly burned up in plasma, radioactive decay of tritium, and calculation uncertainties [5]. Studies in literature show that different concepts examine the *TBR* in fusion reactors. Hernández and Pereslavtsev [6] investigated the solid tritium breeder concept for use in fusion reactors. The *TBR* of all solid tritium breeders was sufficient for operating the reactor sustainably, and Li_3N showed the highest tritium breeding performance. The tritium breeding performance of a solid breeder blanket for (demonstration power station) was examined, and they found that Li_4SiO_4 had the best tritium breeding performance [7].

According to varying cooler thicknesses, neutronic analysis of a magnetic fusion reactor with spherical geometry was performed using FLiBe (Li_2BeF_4) as a coolant [8]. According to the findings, the *TBR* value was sufficient for sustainably operating the reactor, and the optimum coolant thickness was 50 cm. In the 1960s, FLiBe was used as the molten salt (MS) in molten salt reactor experiments (MSRE). The neutronic performance of liquid metals and molten salts in the blanket of a hybrid reactor has been examined [9, 10]. It was observed that a model in which natural lithium was used as a coolant exhibited the highest *TBR* performance. The tritium breeding potential of Li-Sn has been investigated, and it has been determined that when the thick-liquid-breeder concept is applied, the tritium breeding potential of Li-Sn is better than FLiBe [11]. Youssef compared the tritium breeding potential of FLiBe and FLiNaBe, which have favorable melting points, and observed that the tritium production potential of FLiBe was higher than FLiNaBe [12].

The tritium breeding ratio of the fusion-fission hybrid reactors with different molten salts was investigated [13] and the findings of this study determined that the highest *TBR* value was obtained when 90% enriched lithium was used as a coolant in the model. Despite the high *TBR* value obtained in studies using natural or enriched lithium, the radiation damage and energy multiplication factors of the blanket structure of the reactor should be carefully examined. On this basis, FLiBe is a much more appropriate coolant than natural lithium, as it has both a sufficient *TBR* and causes a higher energy multiplication factor and low radiation damage. The effects of varying the lithium enrichment rates and SS304 material used in the first wall on the neutronic performance of the hybrid reactor were examined [14]. The calculations show that the lithium enrichment rate is directly proportional to the total *TBR* and inversely proportional to the displacement per atom (DPA). The vanadium alloy provided the best results in terms of the *TBR* value, and the copper alloy gave the best result in terms of DPA. In this study, the effect of changing the coolers and first wall materials on the neutronic performance of hybrid reactors was examined [15]. The best coolant performance was obtained when FLiBe was used; W-5Re, TZM, T111, and Nb-1Zr were used as the first wall materials. The calculations showed that the worst tritium production performance was obtained when the T111 material was used, whereas the tritium production performance of the other materials was found to be very close to each other. SS304, SS316, ODS, Mo, vanadium, and W were used as the first wall materials in the blanket structure fusion, whereby hybrid reactors were investigated [16]. The highest *TBR* and lowest radiation damage were observed for vanadium and W, respectively. In addition to liquid metals and molten salt coolants in magnetic fusion reactors, gas coolants can be used to make necessary design changes. The effect of the He/LiPb coolants on the neutronic performance of the reactor was examined [17]. Despite sufficient tritium production, the coolant zone of the reactor must be designed for operation at high pressures and temperatures. Wang et al. [18] analyzed the efficiency of CO_2-and He-cooled DEMO fusion power plants and found that helium (He) performed better in terms of gross and net efficiencies. Tillack et al. [19] summarized existing design concepts and parameters for fusion power plants using He as the coolant material and determined that the heat removal capability of He is not worse than that of water in a well-designed system, but noted that an increase in pump power is necessary to work with high-pressure values.

According to the findings obtained from previous studies, the lithium concentration in the coolant materials directly affects tritium production, and neutron breeder isotopes provide a sufficient tritium breeding ratio for autonomous fusion reactor operation. Romatoski and Hu [20] recommended experimental and theoretical property data for candidate fluoride salt coolants for use in nuclear applications. They investigated neutronic and coolant thermophysical properties, such as density, heat capacity, thermal conductivity, and viscosity [20]. In addition, the properties (melting points, densities, neutron multiplier, *TBR*) of the molten salt materials (FLiBe, FLiNaBe, FLiPb), belonging to the family of fluorides with their references in the literature, have been reported [21].

The second element for a successful fusion reactor design is to protect the reactor structure from high-energy neutrons released from the plasma. As such, a layer should be placed between the plasma and reactor layers. The mentioned layer is known as the first wall and can be designed using two essential concepts: solid and liquid. Nevertheless, the solid wall concept is preferred owing to the high neutron damage and wall load in fusion reactors; the liquid wall concept is preferred for hybrid reactors with low wall loads [22, 23]. Tunç et al. [24] investigated the radiation damage parameters of oxide dispersion-strengthened (ODS) steel alloys. According to the results of tritium production, gas production, and nuclear heating calculations, the 12YWT steel

showed the best performance. A comprehensive study on the neutronic performance of reduced activation ferritic/martensitic steels (RAFMs) (such as EUROFER97 and F82H), vanadium alloys, silicon carbide, copper alloys, and stainless steel (SS 316) as the first wall materials has been conducted. V_4Cr_4Ti and $Cu_{0.5}Cr_{0.3}Zr$ exhibited the best tritium breeding, gas production, and DPA performance in this work [4]. In addition to ODS steels, vanadium and copper alloys can also be used as the first wall material in fusion reactors. Muroga [25] used vanadium alloy as the first wall material and FLiBe as the coolant. According to the study results, the reactor produced self-sufficient tritium and the superconductor magnet systems were protected from neutron damage. The Institute of Plasma Physics, Chinese Academy of Sciences (ASIPP), has conducted a series of research and development studies on CLAM as a structural material and related technology. A summary of these studies was presented by Huang et al., primarily covering the composition design, property tests, techniques for joining and coating, and activation analysis, which are corrosion properties of liquid LiPb and irradiation effects from plasma. These studies show that CLAM has some good properties before irradiation from the current test. Huang et al. [26] provided the chemical composition of CLAM, which is based on extensive research from various ongoing international research and development programs on RAFMs.

In contrast to other studies in literature on the neutronic performance of fusion reactors, this study aimed to determine the effect of the material composition and thickness of the first wall on the reactor's neutronic performance, such as tritium breeding materials and first wall material damage. Modeling of a magnetic fusion reactor was completed based on ITER's blanket parameters of the ITER. Stainless steel (SS 316 LN-IG), steel alloy (PM2000 ODS), and CLAM were used as FW materials. The effects of changing the first wall materials and their thickness on the reactor were investigated in the DPA and gas production in the first wall, as well as the *TBR* in the coolant zone and tritium breeding zone. Therefore, in the blanket, fluoride family molten salt materials (FLiBe, FLiNaBe, and FLiPb) as well as the neutron multiplier (Be and Pb) were used as coolants. Lithium oxide (LiO_2) was considered as a tritium production material for comparison.

2 Method

2.1 Description of geometrical model for neutronic calculations

Figure 1 illustrates the MCNP5 geometry output of the simplified model for neutronic analysis of the blanket structure of a magnetic fusion reactor. In this model, the reactor comprised nine layers [27]:

2.1.1 Plasma region inside a D-shaped blanket structure

In this study, deuterium–tritium fusion fuel was used in the magnetic fusion reactor owing to its high-energy potential. In the model where the plasma was homogeneously distributed, the minor radius of the plasma region was 200 cm and its major radius was 620 cm, which was added to the model as a reactor component to preserve the low aspect ratio.

2.1.2 First wall zone

The solid first wall concept was applied in this study. Different stainless steel materials (SS 316 LN-IG, PM2000 ODS, and CLAM) were used as the first wall materials. The effect of the thickness of the first wall (1–5 cm) on the neutronic performance of the reactor was investigated.

2.1.3 Coolant zone

Fluoride family molten salt materials (FLiBe, FLiNaBe, and FLiPb), which have high tritium breeding performance and are also neutron multipliers, were used as coolants in the reactor blanket. The thickness of this layer was chosen to be 50 cm to achieve optimum neutronic performance.

2.1.4 Reflector zones

The first reflector zone (graphite, 10 cm) was added to the reactor model after the coolant zone to reflect the neutrons from the fusion source and send them back to the coolant zone. Graphite was used as a reflector because of the high elastic scattering of neutrons. The second reflector zone (graphite, 20 cm) was also added after the tritium breeding zone to reflect the neutrons and send them back to the tritium breeding zone. In this way, the neutron damage in the magnet layer of the reactor was reduced, and an increase in tritium production and energy multiplication factor values was observed.

2.1.5 Tritium breeding zone

Lithium oxide (LiO_2) was selected as the tritium production material. The layer thickness was determined as 10 cm, and the tritium production potential was increased by adding a reflector zone after this zone.

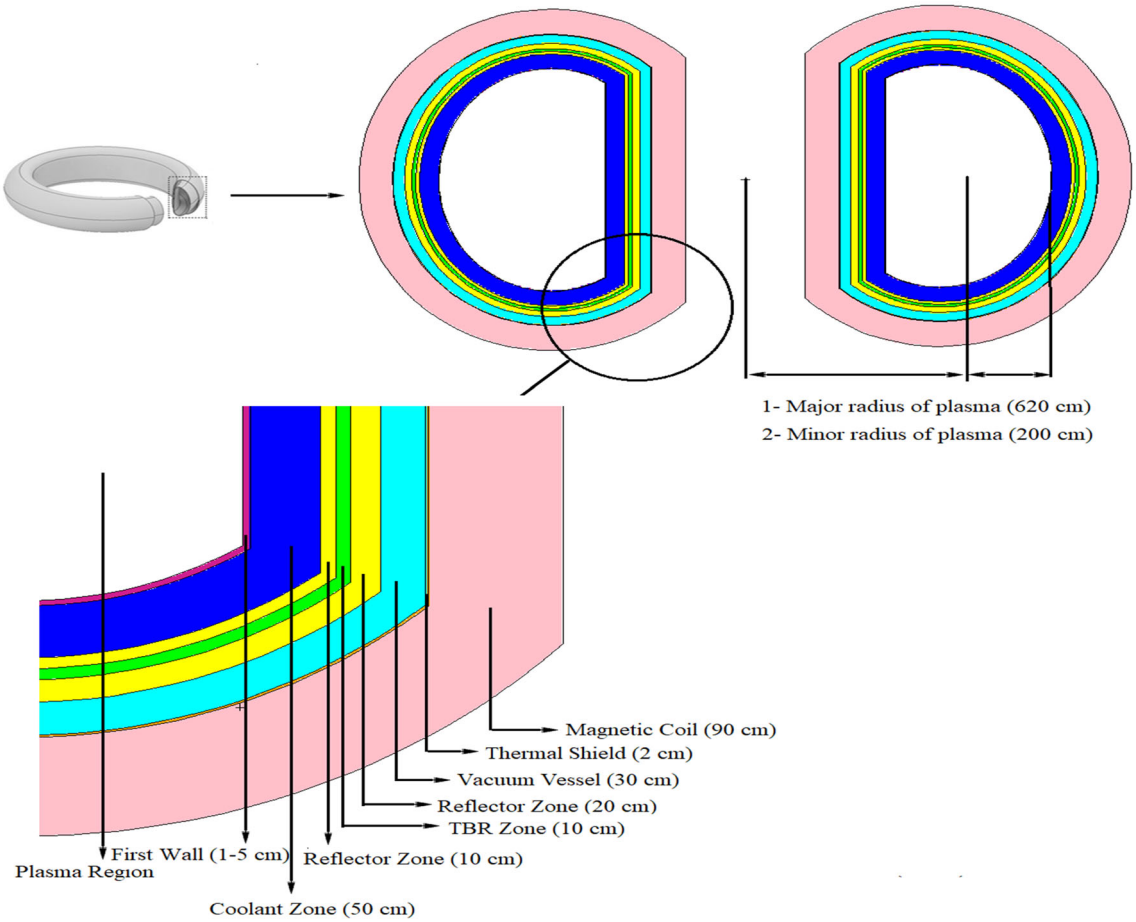

Fig. 1 Blanket structure of investigated magnetic fusion reactor

2.1.6 Vacuum vessel

This is a safety containment barrier that supports plasma stability. It provides a high vacuum environment and electrical resistivity. It has a double structure with electrical and structural continuity [28]. In this study, we assumed that the vacuum vessel was composed of a homogeneous mixture of 60% borated steel (S30467) and 40% water [29]. The thickness of the vacuum vessel was set at 30 cm.

2.1.7 Thermal shield

When the plasma releases heat, conductive heat transfer occurs between blanket components. The thermal shield hampers the heat load required to reach the toroidal field coils. It is composed of stainless-steel panels and panels cooled by helium gas [2]. SS316LN-IG was selected for thermal shielding, and the thickness of the shield was determined to be 2 cm.

2.1.8 Magnetic coil

Plasma limitation in magnetic fusion reactors is accomplished with the help of magnets. The magnets and plasma surrounding the outermost layer of the reactor limit the plasma with a magnetic force according to the limits of the designed reactor. Another function of the magnets is to maintain the plasma in the center of the reactor with magnetic force and prevent it from dispersing. We assumed that magnetic coil was composed of a homogenous mixture of 45% Nb_3Sn, 50% Incoloy 908, and 5% Al_2O_3 [29].

Table 1 lists the atomic densities of the blanket materials in the different zone used in this study. Furthermore, Table 2 shows the isotopic compositions and atomic densities of the candidate materials for the investigated first wall. Moreover, atomic densities of the candidate coolant molten salt materials are given in Table 3.

2.2 Calculation tools

Neutron particle transport calculations were performed using the continuous energy Monte Carlo method with the

Table 1 Atomic densities of the blanket materials

Blanket zone	Material	Specific weight (gr/cm^3)	Nuclide	Nuclei density (atom/barn·cm)
2	First wall candidate	Seen in Table 2		
3	Coolants	Seen in Table 3		
4	Reflector (Graphite)	2.267	C-12	1.13661E-01
5	TBR zone (Lithium oxide)	2.013	Li-6	6.15851E-03
			Li-7	7.49813E-02
			O-16	4.05699E-02
6	Reflector (Graphite)	2.267	C-12	1.13661E-01
7	Vacuum vessel S30467 (60%)	7.8	Fe	5.24159E-02
			C	7.82143E-05
			Mn	1.39364E-03
			Cr	1.74350E-02
			B	9.12492E-03
			Si	8.86414E-04
	H_2O (40%)	1	Ni	1.12828E-02
			H	6.68566E-02
			O	3.34283E-02
8	Thermal shield (SS 316 LN-IG)	8	Fe	5.65101E-02
			C	4.01099E-05
			Mn	1.57845E-03
			P	3.11074E-05
			S	1.50268E-06
			Si	6.86146E-04
			Ni	1.00948E-02
			Cr	1.61217E-02
			Mo	1.20515E-03
			N	2.06424E-04
			Nb	1.03709E-05
			Cu	2.27438E-05
			Co	2.45240E-05
			B	4.01095E-06
			Ta	2.66242E-06
			Ti	1.00576E-05
9	Coil			
	Nb_3Sn (45%)	8.4	Nb	1.71828E-02
			Sn	5.72759E-03
	Al_2O_3 (5%)	3.987	Al	2.35482E-03
			O	3.53223E-03
	Incoloy 908 (50%)	8.17	Fe	1.79278E-02
			Ni	2.05348E-02
			Cr	1.88298E-03
			Nb	7.73161E-04
			Ti	8.93607E-04
			Al	8.47909E-04
			N	3.51351E-06
			Mn	1.83588E-05
			C	2.04811E-05
			Co	4.17419E-05

Table 2 Atomic densities of the first wall candidate materials

Nuclide	Nuclei density (atom/barn·cm)		
	SS 316 LN-IG stainless steel	PM2000 ODS steel alloy	CLAM (China low activation martensitic steel)
Al	–	8.22968E-03	–
B	4.01095E-06	1.20830E-06	–
C	4.01099E-05	3.62493E-05	3.90069E-04
Co	2.45240E-05	7.38789E-06	–
Cr	1.61217E-02	1.58427E-02	8.10948E-03
Cu	2.27438E-05	6.85158E-06	–
Fe	5.65101E-02	5.82026E-02	7.42966E-02
Mn	1.57845E-03	8.71764E-05	3.83760E-04
Mo	1.20515E-03	4.53768E-06	–
N	2.06424E-04	8.70346E-06	6.69159E-05
Nb	1.03708E-05	–	–
Ni	1.00948E-02	7.41810E-06	–
O	–	6.80340E-04	–
P	3.11074E-05	2.81133E-06	4.53779E-06
S	1.50268E-06	2.85190E-06	2.92272E-06
Si	6.86146E-04	6.20104E-05	1.66819E-05
Ta	2.66242E-06	–	3.88381E-05
Ti	1.00576E-05	4.09313E-04	5.86275E-06
V	–	–	1.83939E-04
W	–	9.47325E-06	3.82271E-04
Y	–	1.81196E-04	–
Zr	–	4.77276E-06	–
Total	8.65498E-02	8.37873E-02	8.38818E-02

Table 3 Atomic densities of the candidate coolant materials

Nuclide	Nuclei density (atom/barn·cm)		
	FLiBe LiF (67%) + BeF_2 (33%)	FLiPb LiF (40%) + PbF_2 (60%)	FLiNaBe LiF (35%)-NaF (27%)-BeF_2 (38%)
Density	1.94	3.545	2.0
Li-6	1.80234E-03	4.11519E-04	8.35829E-04
Li-7	2.19439E-02	5.01034E-03	1.01764E-02
Be-9	1.16959E-02	–	1.19562E-02
F-19	4.71381E-02	2.16875E-02	4.34197E-02
Na-23	–	–	8.49516E-03
Pb-206	–	2.07386E-03	–
Pb-207	–	1.79735E-03	–
Pb-208	–	4.26158E-03	–
Total	8.25802E-02	3.52421E-02	7.48833E-02

well-known 3D code MCNP5 [30]. MCNP5 allows for a unique geometric definition limited only by the available computing power band, which uses the built-in continuous energy nuclear and atomic data libraries such as the Evaluated Nuclear Data File (ENDF) system [31]. ENDF/B-V and ENDF/B-VI are nuclear data files evaluated in a US study coordinated by the National Nuclear Data Center at Brookhaven National Laboratory [32]. ENDF/B-V [33] and ENDF/B-VI [34] are neutron energy regimes that are 10^{-11} MeV to 20 MeV for all isotopes, and 150 MeV for some isotopes. In addition, the activity cross-section data library CLAW-IV [35] was used for atomic displacement

cross-sections of FW structural materials to evaluate both the DPA values and gas production.

An interface computer program written in the FORTRAN 90 language to evaluate the MCNP5 outputs was developed for the fusion reactor blanket. Figure 2 shows the flowchart of the interface code for the assessment of the MCNP5 output, entitled MCNPAS (MCNP Assessment Code) [36]. In the first step, with the stochastic MCNP5/MCNPAS code, the MCNP5 code calculates the neutron fluxes and reaction rates in the cells and surfaces [37]. In the second step, the interface code reads the required data from the output and activity cross-section data library, CLAW-IV. Thereafter, the interface code calculates neutronic performance parameters such as *TBR*, DPA, gas production, and nuclear heating.

3 Results and discussion

3.1 Fusion blanket performance

Fluoride family molten salt materials (FLiBe, FLiNaBe, FLiPb) as well as the neutron multiplier and lithium oxide (LiO_2) were considered the coolant and tritium production material in the blanket, respectively. We performed calculations to compare the fusion blanket performance.

3.1.1 Tritium breeding ratio

Tritium is an important and hazardous material. Because tritium is difficult to obtain and degrades with a half-life of 12.3 years, the quantity produced must be as much as is needed to be consumed. Therefore, one triton must be bred in the blanket for every triton consumed in the D–T fusion reaction. Thus, the fusion blanket must contain tritium breeding material. Tritium can be produced by contact with lithium during the fusion reaction. The neutrons escaping the plasma must interact with the lithium contained in the blanket to produce tritium. Therefore, the only viable choice is Li, which is naturally composed of 92.41% ^{7}Li and 7.59% ^{6}Li. Both isotopes breed tritium, but ^{6}Li breeds much more than ^{7}Li does. In other words, the tritium reaction cross-section increases with decreasing neutron energy, namely thermal neutrons, whereas the cross-sections of (^{7}Li, n) are much lower. Neutrons produce tritium via the following reactions for both isotopes:

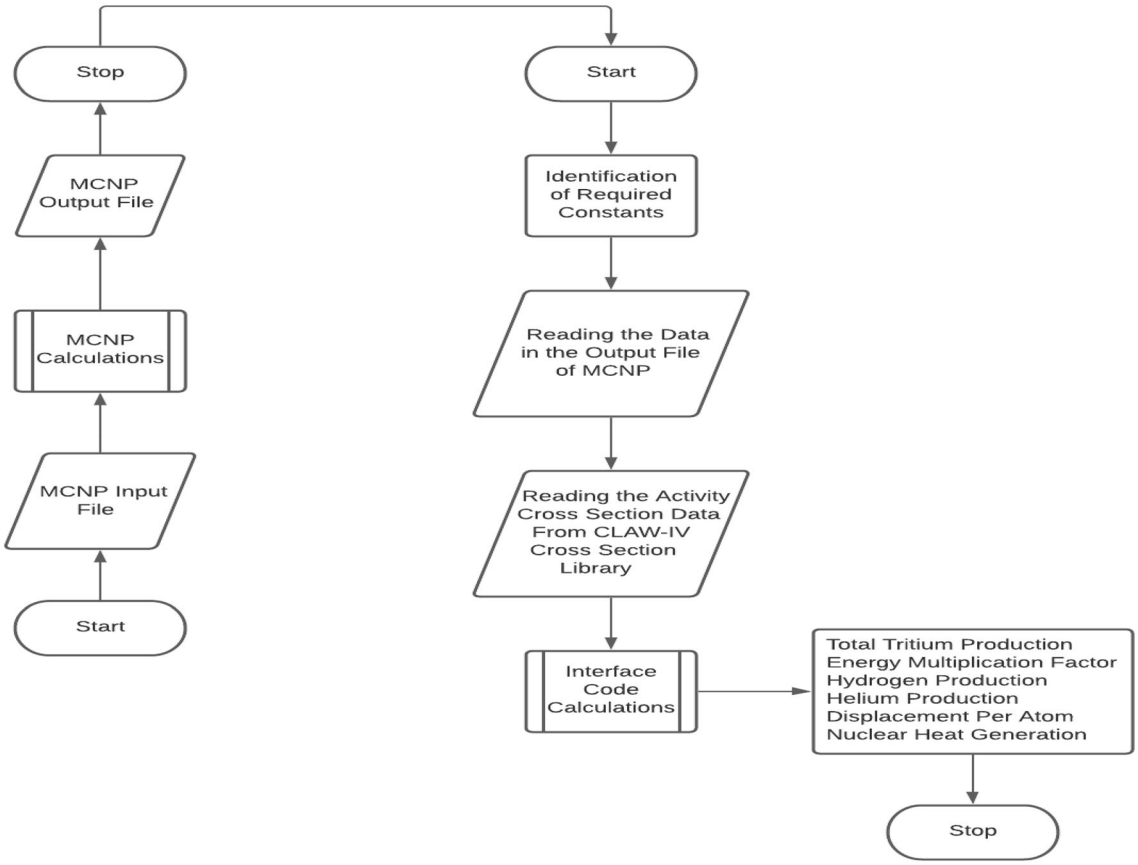

Fig. 2 Flowchart of the problem solution

$$^{6}_{3}\mathrm{Li} + \mathrm{n} \rightarrow {}^{4}_{2}\mathrm{He} + {}^{3}_{1}\mathrm{H} + 4.8\,\mathrm{MeV}, \quad (1)$$

$$^{7}_{3}\mathrm{Li} + \mathrm{n} \rightarrow {}^{4}_{2}\mathrm{He} + {}^{3}_{1}\mathrm{H} + \mathrm{n} - 2.5\,\mathrm{MeV}. \quad (2)$$

As can be observed from the reactions, one neutron produces only one tritium atom in the (^{6}Li, n) reaction. In addition, in Eq. 1, the exoenergic neutron absorption in ^{6}Li occurs in tritium breeding and an important heat effect is generated. A neutron multiplier was added to increase tritium breeding efficiency. Beryllium (Be) is mainly a neutron multiplier, and (Pb) was also considered in some concepts of tritium breeding blankets [38].

As shown in Fig. 3, high-energy neutrons (14 MeV) have a higher cross-section of Pb(n,2n), whereas lower-energy neutrons have a higher cross-section of Be(n,2n) [39]. In addition, as shown in Fig. 4, the coolant zone exhibits a high-energy neutron spectrum. Therefore, lead-containing coolants increase the efficiency of tritium breeding. Hence, we investigated the *TBR* production in two regions of the blanket layer. These effects are also clearly seen in Fig. 5 when comparing the *TBR* performance of the coolants. The *TBR* production rates in these two regions are shown in Fig. 5. These were the coolant and tritium breeding zones, respectively. As shown in Fig. 5, the contribution of the lead-containing (Pb) coolant (FLiPb) to the total TBR shows that there is a sharp increase in tritium production in the tritium breeding zone, namely the LiO_2 zone. Among the three different first wall materials, the best performance of the total *TBR* was obtained for the FLiPb coolant. Moreover, when the first wall was 2 cm for all materials, the *TBR* value produced in the coolant zone was sufficient.

In addition, to resist fusion plasma damage and protect the blanket, the first wall, which is the first layer of the blanket on the plasma side, must be composed of steel with a strong structure. This affects the reaching of high-density metal fusion neutrons to the *TBR* region and the amount of *TBR* production. To measure the effect of the first wall thickness, the *TBR* was calculated for various materials used on the first wall. Because more neutrons were moderated after travelling through the thick first wall, to observe this effect, three different materials were used as the first wall material by changing from 1 to 5 cm.

As can be seen from Fig. 6, in the first wall material (SS 316 LN-IG), as the first wall material thickens from 1 to 5 cm, the *TBR* values decrease from 1.20 to 1.00, from 1.28 to 1.00, and from 1.08 to 0.94 for the FLiBe, FLiPb, and FLiNaBe coolants, respectively. When examining the values for the first wall material (SS 316 LN-IG), the highest reduction in the *TBR* was 22% for FLiPb coolant. In the same examination, in the first wall material (PM2000 ODS), as the first wall material thickened from 1 to 5 cm, the *TBR* values decrease from 1.22 to 1.10, from 1.31 to 1.09, and from 1.10 to 1.02 for the FLiBe, FLiPb, and FLiNaBe coolants, respectively. When examining the values for the first wall material (SS 316 LN-IG), the highest reduction in the *TBR* was 17% for FLiPb coolant. For the first wall material (CLAM), as the first wall material thickens from 1 to 5 cm, the *TBR* values decrease from 1.22 to 1.08, from 1.30 to 1.04, and from 1.09 to 0.98 for FLiBe coolant, FLiPb coolant, and FLiNaBe coolant, respectively. When examining the values for the first wall material (SS 316 LN-IG), the highest reduction in the *TBR* was 20% for FLiPb coolant. In terms of the *TBR*, the best performance was obtained for the 1 cm first wall material PM2000 ODS.

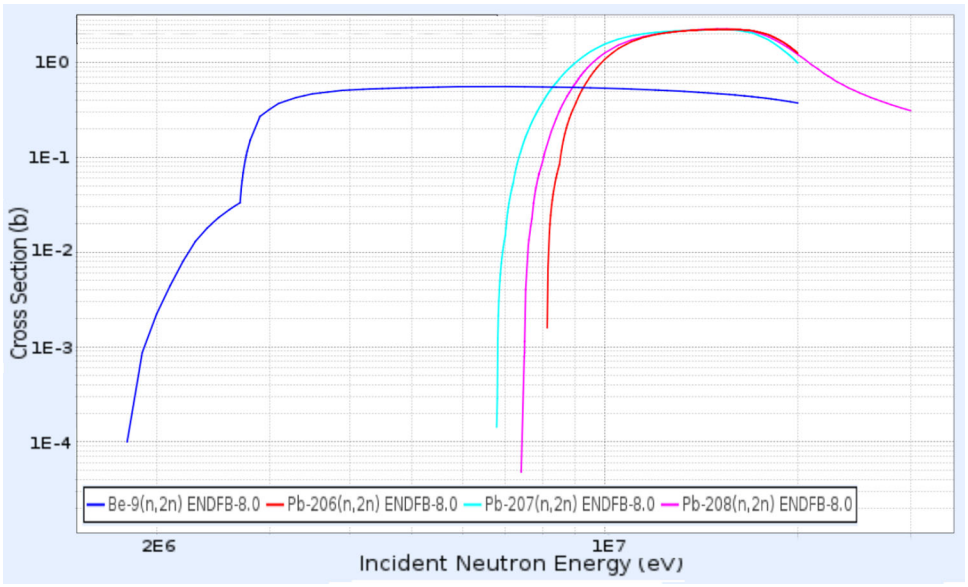

Fig. 3 Cross-section of Be(n,2n) and Pb(n,2n) at the KAERI Nuclear Data Center

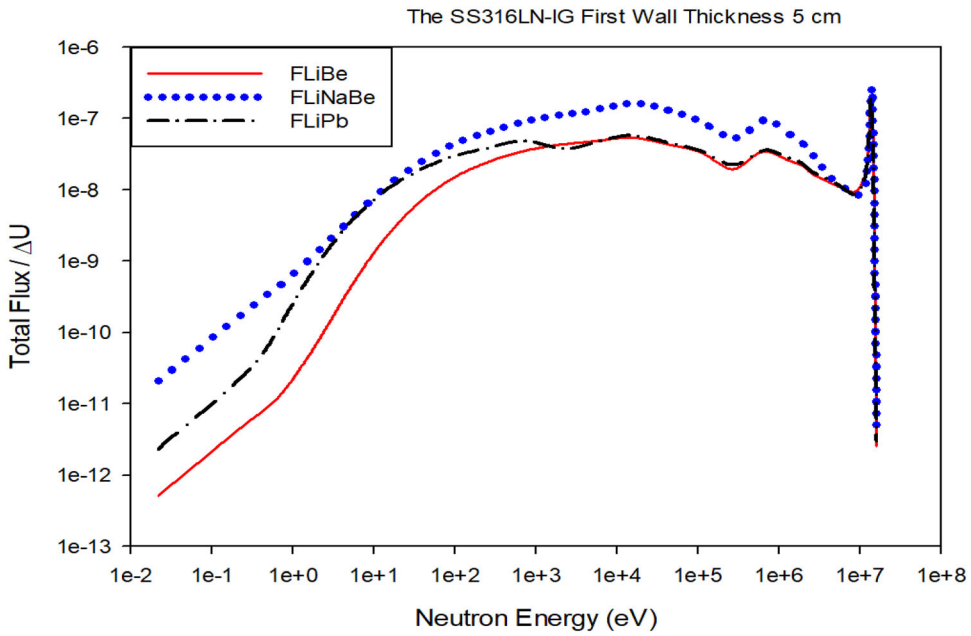

Fig. 4 The coolants neutron spectrum at coolant region (with 5 cm SS316LN-IG first wall thickness)

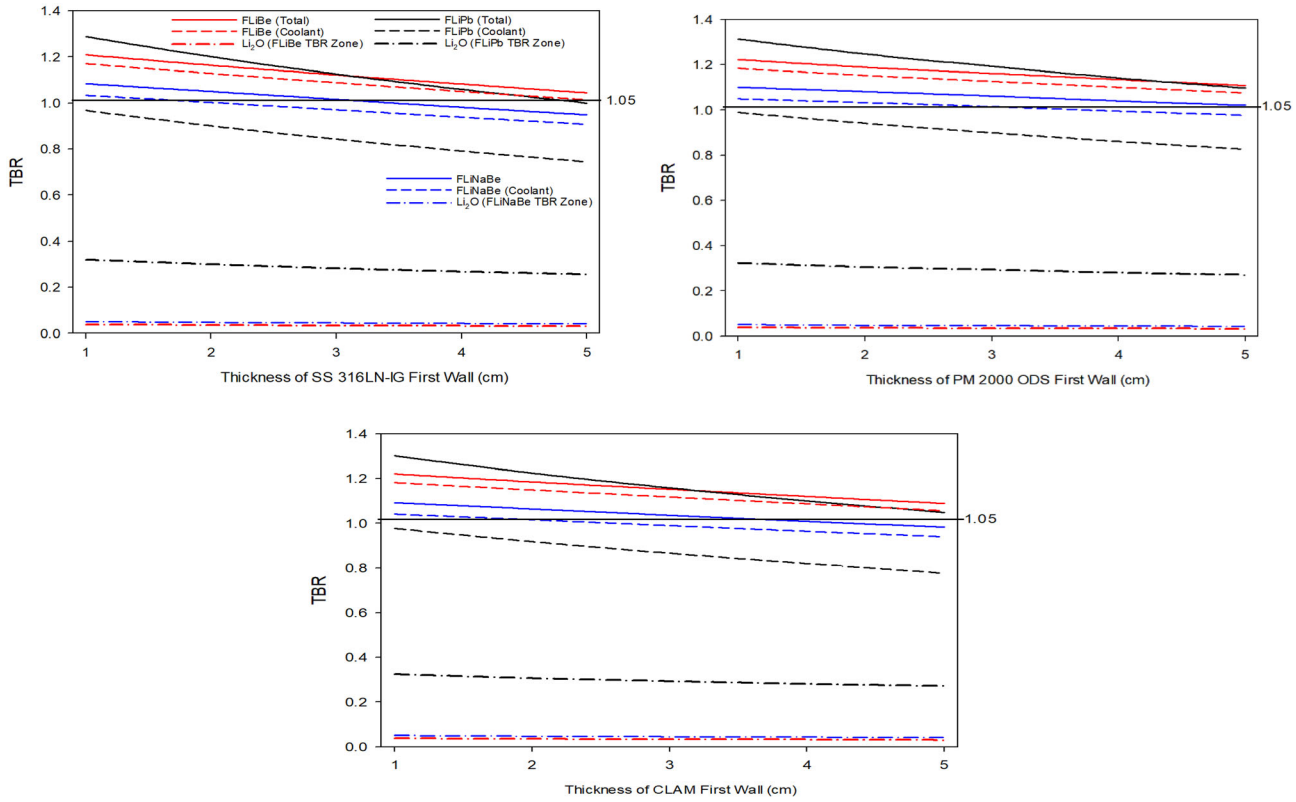

Fig. 5 The change in the tritium breeding ratio with respect to thickness for first wall materials

Sufficient tritium production in the fusion reactor blanket must be maintained to sustain the reactor. The figures are useful for evaluating the effects of the first wall thickness on the overall production of tritium.

3.1.2 Energy multiplication factor

Energy multiplication through various neutronic reactions in the blanket is an important performance parameter for fusion reactors. In the blanket of a fusion reactor, nearly

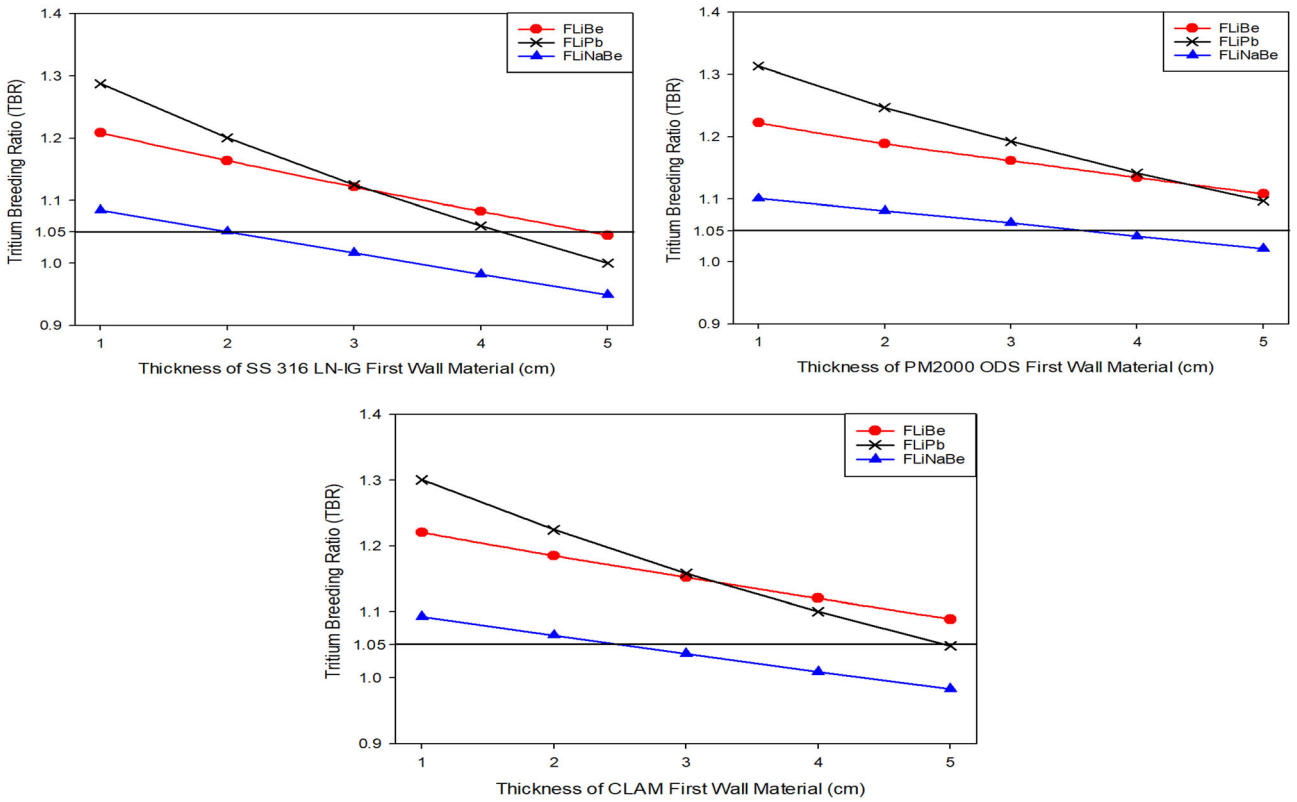

Fig. 6 The change in the tritium breeding ratio with respect to thickness for first wall materials

all the kinetic energy of 14 MeV neutrons is converted into useful heat energy by multiple scattering. The multiplication factor (M) was calculated using Eq. 3.

$$M = 1 + \frac{[(\Sigma_{\text{tritium}}(^{6}_{3}\text{Li}) \times 4.786) - (\Sigma_{\text{tritium}}(^{7}_{3}\text{Li}) \times 2.467)]\,\text{MeV}}{14.1\,\text{MeV}} \quad (3)$$

Per Eq. 1, the exoenergic neutron absorption in ^{6}Li occurs in tritium breeding and an important heat effect is generated in the coolant and tritium breeding zones. In addition, the addition of the neutron multipliers Be(n,2n) and Pb(n,2n) to the coolant increases the energy multiplication factor. Moreover, the γ-emissions in the first wall material and coolants resulting from the (n, γ) reactions contribute to overall heat energy production. Figure 7 illustrates the change in M with respect to the thicknesses of the first wall materials and coolants. The highest energy multiplication is observed with the FLiPb coolant, which is directly related to the neutron multiplier and intense γ emission in lead and occurs via multiple inelastic neutron scattering reactions. As shown in Figs. 6 and 7, both the M factor and TBR are the highest owing to neutron multiplication in the FLiPb coolant; additionally, the M and TBR values decrease as the thickness of the first wall material increases..

3.2 Radiation damage in the first wall

In the fusion reactor, the first wall (FW) was exposed to large amounts of plasma and electromagnetic radiation. At the same time, the first wall protected the blanket from the plasma. Additionally, the first wall (FW) was exposed to 14 MeV high-energy neutrons released from the DT reaction. High-energy neutrons caused nuclear reactions in the first wall in terms of material damage, a criterion of the fusion reactor structure. It is known that the most important parameters are DPA and gas production, such as production of He and H.

Radiation damage, a design concept for fusion energy reactors, limits the lifetime of the FW structure to one full power year (FPY), which means that the FW material must be replaced every year. In this study, 100 DPA/FPY was selected as the DPA limit criterion for FW structural materials [40, 41]. Radiation damage beyond certain limits warrants the replacement of the first wall material. In addition, according to the literature, the acceptable limit for helium production was chosen as 500 appm (atomic parts per million) [42, 43]. When the first wall radiation was evaluated in terms of damage criteria, we observed that the first wall thickness used in this study was sufficient. However, when evaluated in terms of the fusion reactor blanket as a whole, we found that the FLiBe and FLiPb

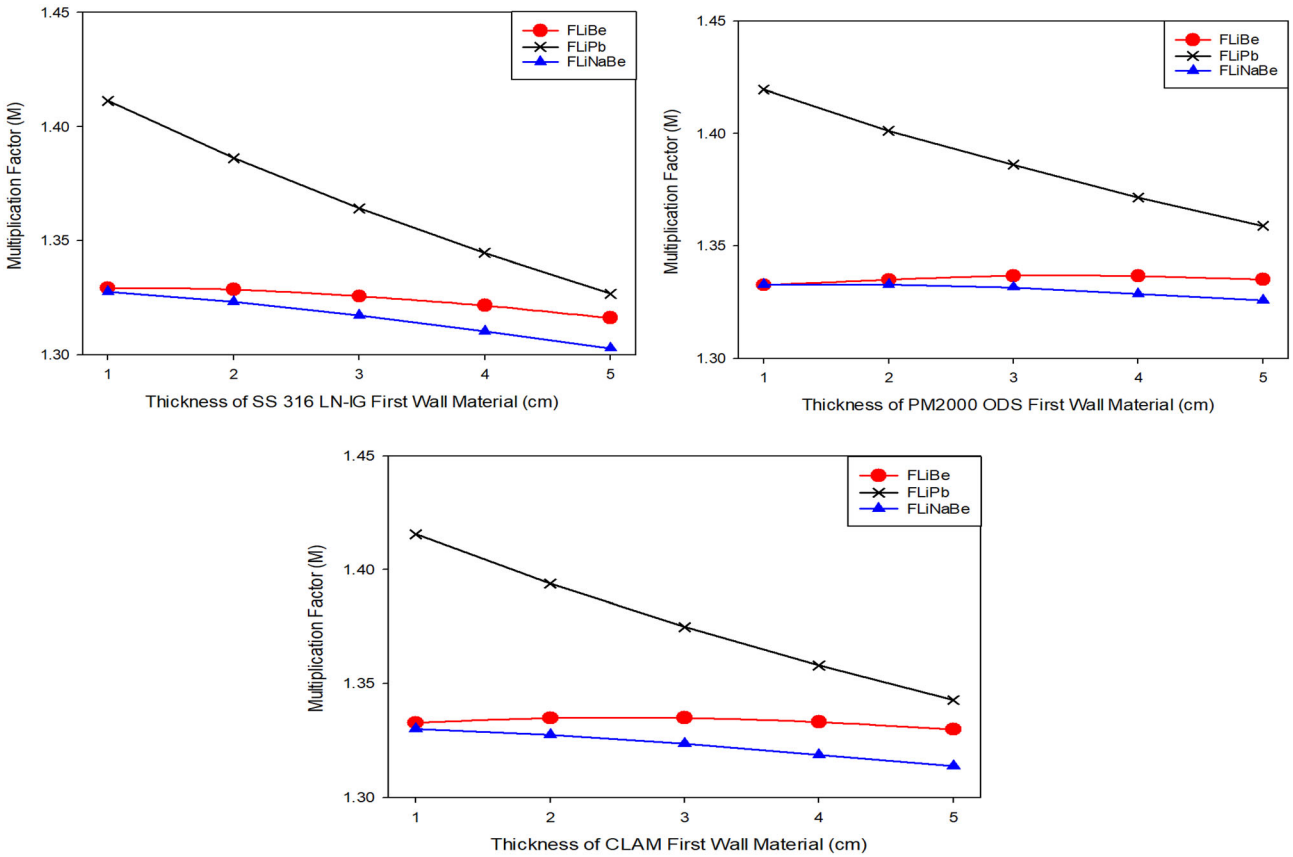

Fig. 7 The change in the multiplication factor with respect to thickness for first wall materials and coolants

coolants, in which ODS steel is used together, provide the best performance, especially when considering the production of *TBR*, as shown in Fig. 6.

3.2.1 Displacement per atom

The DPA is expressed as a measure of the damage caused to the atomic crystal structure of a substance via bombardment with energy particles. In other words, the number of times each atom is separated from its location in the crystal by radiation. The displacement per atom in a lattice structure is called DPA. In other words, one DPA is equivalent to displacing all atoms from their lattice sites. In the first wall calculations, the DPA is expressed as a probability. This possibility is called the DPA cross-section. Neutrons that cause DPAs are usually those with energies greater than 1 MeV. Thermal neutrons do not cause DPAs. The cross-section for the processes of neutron displacement damage is generally in the range of 1–10 barns [38].

Three types of first wall materials were considered for the first wall performance. However, the coolants behind the first wall also affected its structure. This is because the coolants contain neutron multiplier isotopes. Thus, both factors should be considered when evaluating the DPA performance. As shown in Fig. 8, during first wall damage, the DPA is higher when the FLiPb coolant is used because high-energy neutrons (14 MeV) have a higher Pb(n,2n) cross-section and high neutron multiplier. In other words, as the number of neutrons in the material increases, more DPAs occur on the first wall than in the FLiBe and FLiNaBe coolants. In addition, because Fe and Cr have the highest content of all the first wall materials, one can say that the DPA damages of the first wall materials are approximately similar.

Figure 8 illustrates the change in the DPA values with respect to the thickness of the first wall material and the three different coolants. Neutron moderation in lithium, the lightest coolant element, decreases the DPA. Neutron multiplication in FLiPb is higher than that in FLiBe and FLiNaBe because high-energy neutrons (14 MeV) have a higher cross-section of Pb(n,2n), whereas thermal neutrons have a higher cross-section of Be(n,2n). Therefore, as observed in Fig. 8, regarding the first wall materials, the lead-containing FLiPb coolant had the highest DPA values. In the first wall material (SS 316 LN-IG), as the first wall material thickens from 1 to 5 cm, the DPA values decreased from 7.17 to 5.66, from 7.95 to 6.09, and from

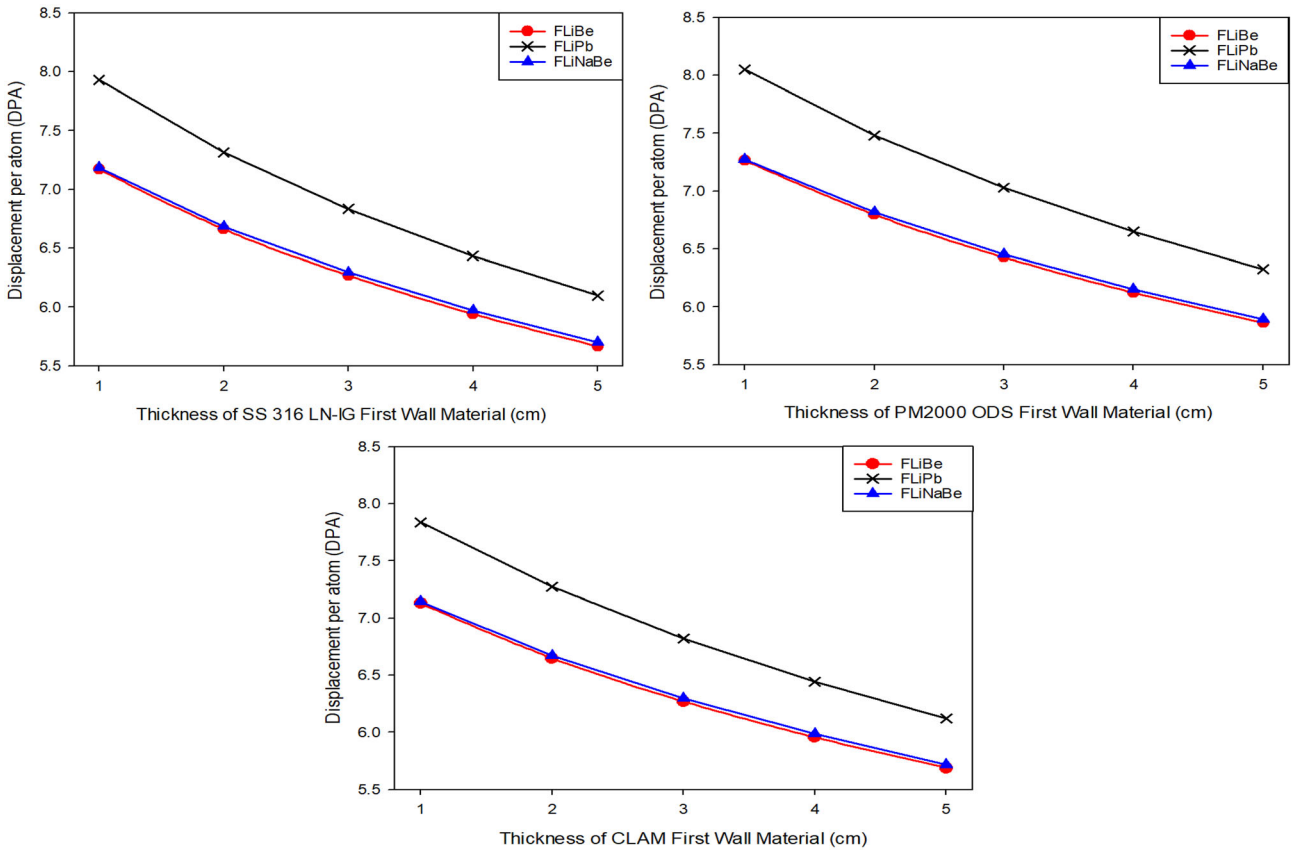

Fig. 8 The change in the displacement per atom with respect to thickness for first wall materials

7.18 to 5.69 for the FLiBe coolant, FLiPb coolant, and FLiNaBe coolant, respectively. . When examining the values for the first wall material (SS 316 LN-IG), the highest reduction in the DPA was 23% for the FLiPb coolant. In the same examination, in the first wall material (PM2000 ODS), as the first wall material thickens from 1 to 5 cm, the DPA values decreased from 7.26 to 5.86, from 8.05 to 6.32, and from 7.27 to 5.89 for the FLiBe coolant, FLiPb coolant, and FLiNaBe coolant, respectively. When examining the values for the first wall material (SS 316 LN-IG), the highest reduction in the DPA was 21% for the FLiPb coolant. For the first wall material (CLAM), as the first wall material thickens from 1 to 5 cm, the DPA values decreased from 7.12 to 5.68, from 7.83 to 6.12, and from 7.14 to 5.71 for the FLiBe coolant, FLiPb coolant, and FLiNaBe coolant, respectively. When examining the values for the first wall material (SS 316 LN-IG), the highest reduction in the DPA was 22% for FLiPb coolant.

3.2.2 Gas production

In contrast to production of helium (He), a higher production of hydrogen (H) was obtained for the investigated FW structures because of the higher σ(n,p) cross-section than σ(n,α) and lower (n,p) threshold energies than (n,α) [44].

Figure 9 shows the change in H production with respect to the thickness of the first wall materials. H production decreases as the material thickness increases, and has approximately the same values per full power year for all first wall materials. As shown in Fig. 9, the lowest H production values were obtained for the FLiPb coolant, and the highest H-production values were obtained for the FLiBe and FLiNaBe coolants, which had almost the same H production values. As shown in Fig. 9, , the values obtained for the FLiBe and FLiNaBe coolants were slightly higher than the ones for FLiPb. The highest H production values were 219.2, 175.1, and 179.5 appm/FPW and the lowest were 140.3, 114.6, and 116.2 appm/FPW using FLiBe and FLiNaBe coolant for SS316, ODS, and CLAM, respectively. The reductions in the H production value were 35%. Because all the hydrogen isotopes produced by the (n, p), (n, d), and (n, t) reactions diffuse out of the metallic lattice or form metal hybrids, H production values were not considered in this study. Therefore, no damage limit was chosen for H production.

Figure 10 shows the change in He production with respect to the thickness of the first wall and coolant

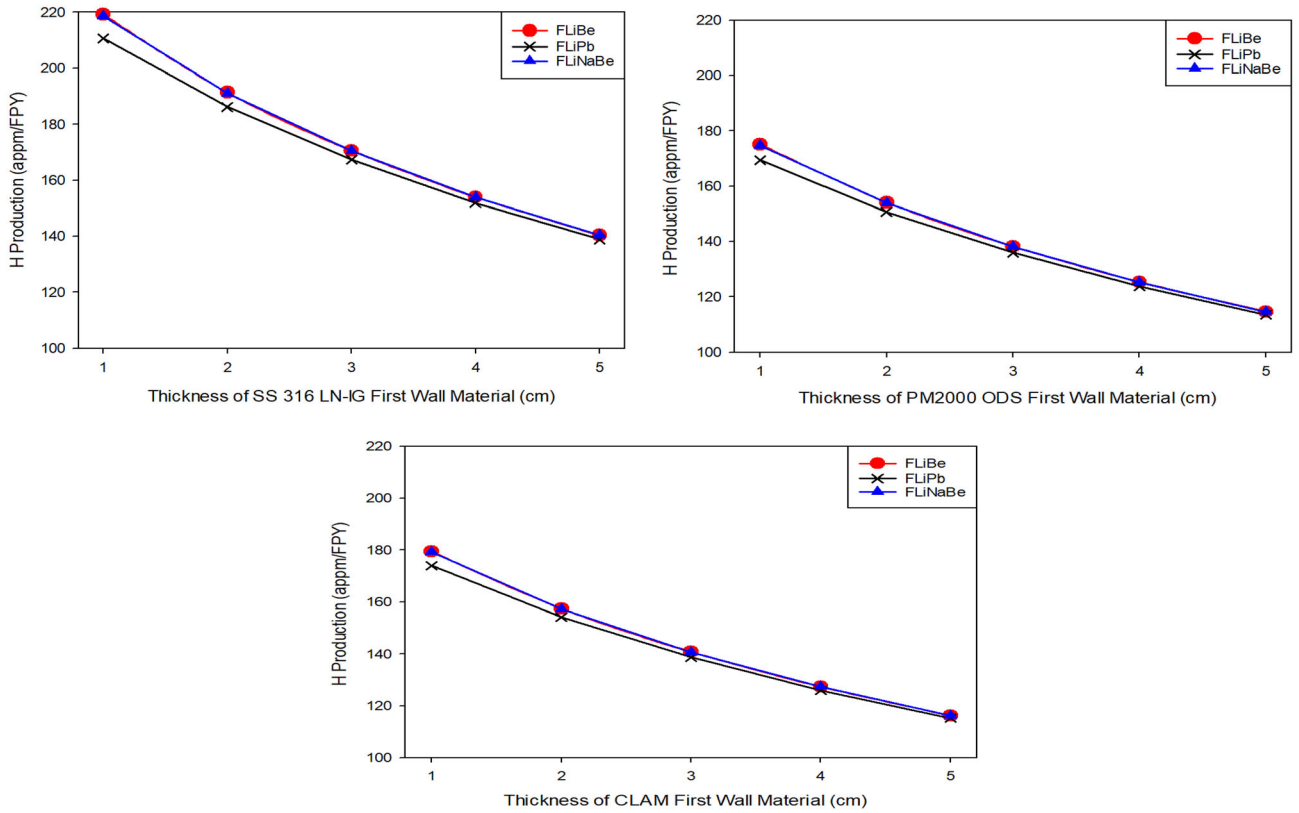

Fig. 9 The change in hydrogen production with respect to thickness for first wall materials

materials. The He production decreases as the material thickness increases, and has approximately the same values per full power year for all first wall materials. The same situation can be seen when overall Fig. 10 is examined, the lowest He production values were obtained for FLiPb coolant; the highest He-production values were obtained almost the same for FLiBe and FLiNaBe coolants. The FLiBe and FLiNaBe coolants were slightly higher than these values. They decreased slowly from 83.5, 81.7, and 69.3 appm/FPW to 53.1, 53.3, and 44.7 appm/FPW using the FLiBe and FLiNaBe coolant for SS316, ODS, and CLAM, respectively.

As clearly observed in Figs. 9 and 10, H production is considerably higher than He production, which is related to the lower threshold energy and higher hydrogen cross-sections.

3.2.3 Structural lifetime

The determining time for replacing the first wall is known as the DPA breakpoint. Many studies have been conducted between the DPA values of 100 and 1000 atomic particles per million (appm) as the design limit for candidate structural materials [42, 43, 45–48]. According to these references, a more conservative limit of 100 DPA was applied for radiation damage in this study. Figure 11 shows the DPA values for the investigated FW structural material thickness and the three different coolants as a function of the years. When Fig. 11 is examined overall regarding the DPA limit, the FLiPb coolant achieved DPA damage with the lowest lifetime. As the first wall material thickens from 1 to 5 cm, the DPA damages start from 12.6, 12.4, and 12.7 years to 16.3, 15.8, and 16.3 years with FLiBe, for the SS-316, ODS, and CLAM structure, respectively.

In addition, the α-particles (n,α) remain in the metal and produce bubbles of helium gas, that is, He production. In this study, a conservative design limit of He production was suggested to be 500 atomic parts per million [appm] as a criterion for helium production in the FW structure. Figure 12 shows the change in structural lifetime with respect to the thickness for the first wall materials with three different coolants regarding the He-production limit. As shown in Fig. 12, almost identical lifetime values were observed. These replacement periods ranged from 6 to 11 years.

The He/DPA ratio (He/DPA) determines whether the damage to the first wall is primarily owing to the DPA or He production. This value is 5, as the limit value for helium is 500 appm, and for the DPA, the limit value is 100 appm.

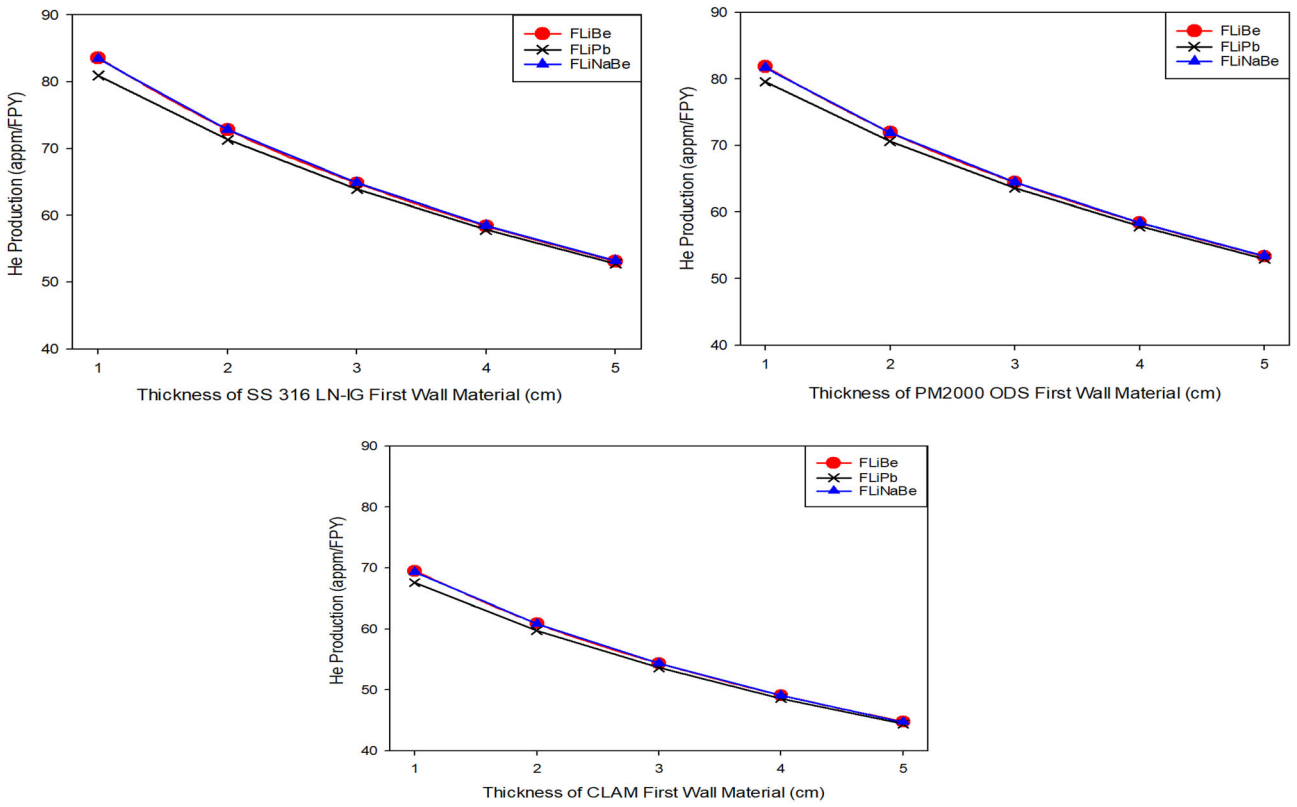

Fig. 10 The change in helium production with respect to thickness for first wall materials

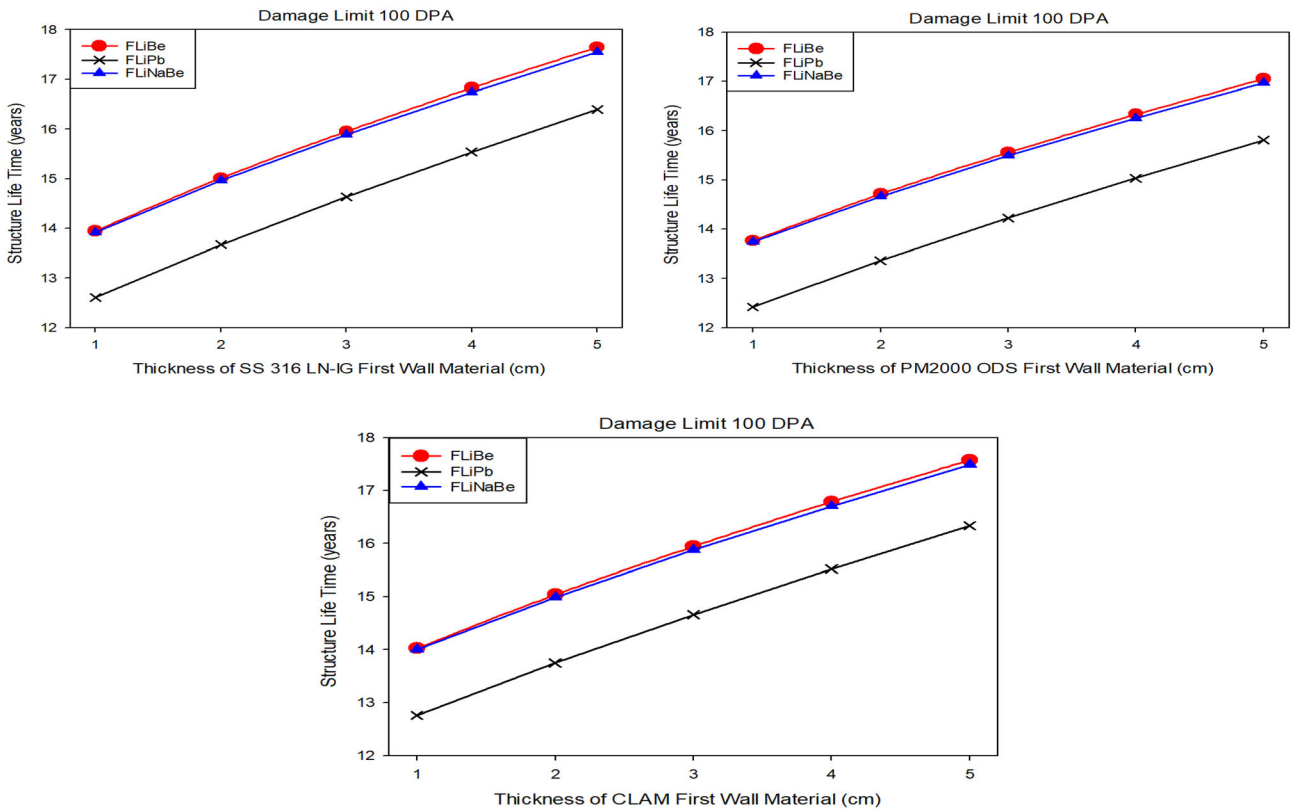

Fig. 11 The change in structural lifetime with respect to thickness for first wall materials regarding the DPA limit

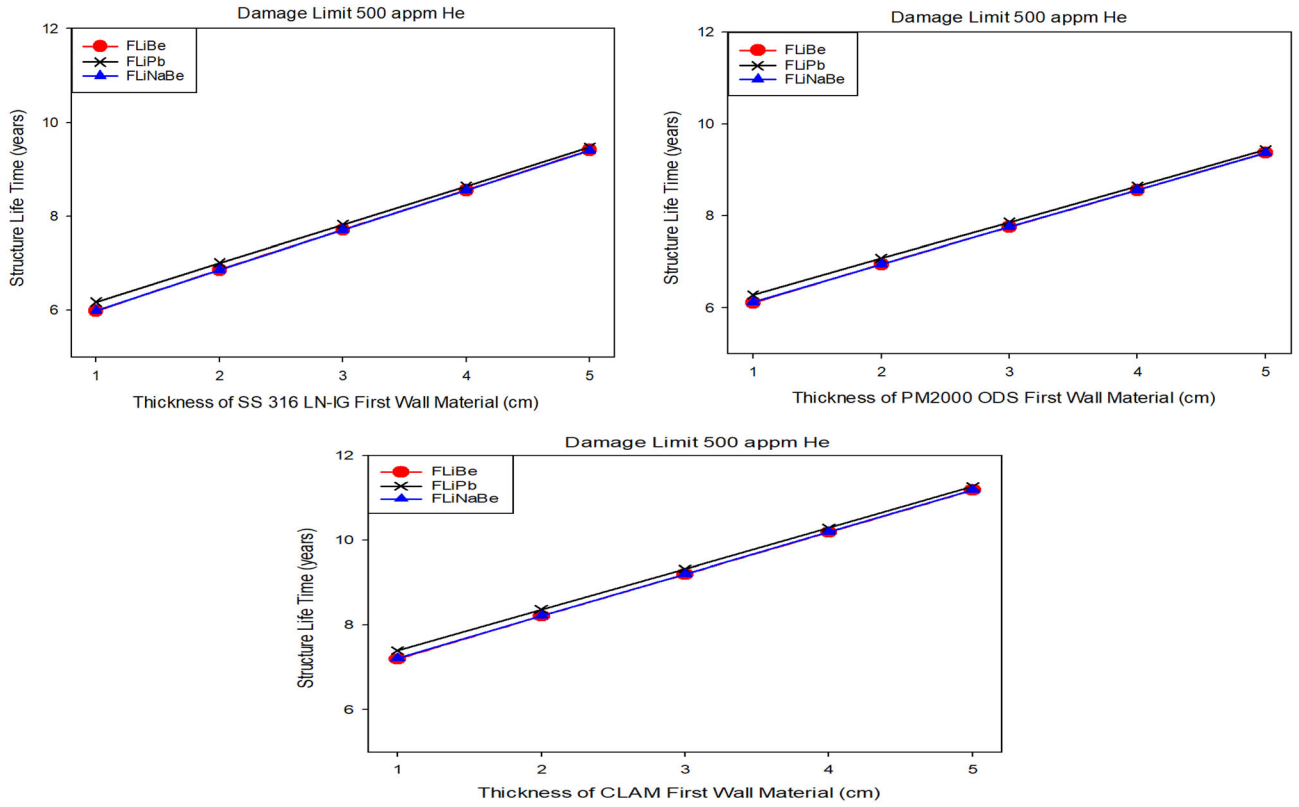

Fig. 12 The change in structural lifetime with respect to thickness for first wall materials regarding He limit

If the He/DPA value is less than 5, the DPA is first, and if it is greater than five, He production starts to damage first. Table 4 shows that the He/DPA ratio is above 5 for all FW materials and molten salt coolants. In addition, the DPA and He structural lifetimes and He/DPA ratio with respect to different first wall materials and coolants can be determined. Moreover, the overall results in Table 4 differ from the DPA damage meaning, which leads to the highest helium production and gas bubbles built into the metallic crystal for all FW materials. In light of these explanations, He production should be considered as the factor determining the replacement of FW material in this study.

4 Conclusion

In a fusion reactor, the FW suffers the highest degree of material damage in the top part of the blanket facing directly into the fusion chamber. In addition, maintenance and replacement of FW are very difficult and costly and require long plant shutdown times. Additionally, in FW, low levels of DPAs and gas production (He and H) are essential for continuous and prolonged plant uptimes. Therefore, in this study, we modeled a magnetic fusion reactor was based on the blanket parameters of the ITER. SS 316 LN-IG, PM2000 ODS, and CLAM were used as FW materials. Fluoride family molten salt materials (FLiBe, FLiNaBe, FLiPb) and lithium oxide (LiO_2) were considered as the coolant and tritium production material in the blanket, respectively. The effects of changing the first wall materials and their thicknesses on the reactor were investigated for DPAs and gas production in the first wall and the TBR in the coolant zone and tritium breeding zone.

Neutronic calculations were performed via the Monte Carlo method using the widely applied 3D particle transport code MCNP with built-in continuous energy nuclear and activity cross-section data libraries, the Evaluated Nuclear Data File (ENDF) system (ENDF/B-V and ENDF/B-VI), and CLAW-IV. The most recent version, MCNP, was successfully applied to evaluate neutronic parameters. This means that it is generally considered to be a good predictor of processes and systems.

The main results are summarized as follows:

- The lead-containing coolant increases tritium breeding efficiency, and the contribution of the lead-containing (Pb) coolant (FLiPb) to the total *TBR* clearly shows a sharp increase in tritium production in the tritium cultivation zone.
- Both the *M* factor and *TBR* were the highest in the FLiPb coolant; additionally, the *M* and *TBR* values

Table 4 DPA and He Structural Lifetime and He/DPA ratio with respect to Different First Wall Materials and Coolants

First wall \ Coolants	DPA-lifetime (Year)			He-lifetime (Year)			He/DPA		
	FLiBe	FLiPb	FLiNaBe	FLiBe	FLiPb	FLiNaBe	FLiBe	FLiPb	FLiNaBe
SS 316 LN-IG (1 cm)	13.944	12.608	13.914	5.984	6.175	5.993	11.651	10.209	11.609
SS 316 LN-IG (2 cm)	15.012	13.669	14.961	6.863	7.008	6.864	10.938	9.752	10.899
SS 316 LN-IG (3 cm)	15.953	14.631	15.885	7.712	7.821	7.708	10.343	9.354	10.304
SS 316 LN-IG (4 cm)	16.830	15.539	16.740	8.560	8.643	8.551	9.831	8.990	9.788
SS 316 LN-IG (5 cm)	17.647	16.397	17.545	9.412	9.475	9.399	9.374	8.652	9.334
PM2000 ODS (1 cm)	13.766	12.422	13.745	6.110	6.282	6.120	11.266	9.886	11.229
PM2000 ODS (2 cm)	14.715	13.366	14.666	6.947	7.078	6.951	10.591	9.443	10.549
PM2000 ODS (3 cm)	15.559	14.224	15.491	7.755	7.859	7.756	10.031	9.050	9.987
PM2000 ODS (4 cm)	16.332	15.038	16.249	8.562	8.643	8.559	9.538	8.699	9.493
PM2000 ODS (5 cm)	17.051	15.809	16.972	9.375	9.439	9.370	9.095	8.374	9.057
CLAM (1 cm)	14.026	12.757	14.002	7.195	7.398	7.210	9.748	8.622	9.710
CLAM (2 cm)	15.038	13.749	14.992	8.213	8.371	8.222	9.156	8.212	9.117
CLAM (3 cm)	15.946	14.660	15.877	9.198	9.324	9.205	8.668	7.861	8.624
CLAM (4 cm)	16.789	15.521	16.705	10.187	10.289	10.191	8.240	7.542	8.196
CLAM (5 cm)	17.578	16.337	17.492	11.181	11.268	11.184	7.861	7.249	7.820

decreased as the thickness of the first wall material increased.

- The first wall was 2 cm for all materials, the *TBR* value produced in the coolant zone was sufficient, and the best performance was obtained for the 1 cm first wall material PM2000 ODS.
- The lead-containing FLiPb coolant had the highest DPA value for the first wall material.
- Because Fe and Cr have the highest content of all the first wall materials, one can say that the DPA damages of the first wall materials are approximately similar.
- Higher H production than He production was obtained for the investigated FW structures.
- Because all the hydrogen isotopes diffuse out of the metallic lattice or form metal hybrids, H production values were not taken into consideration in this study.
- The lowest He production values were obtained for the FLiPb coolant, and the highest He production values were obtained for the FLiBe and FLiNaBe coolants.
- He production was considered the factor determining the replacement of FW material due to the He/DPA ratio.
- Replacement periods were obtained between 6 and 11 years for the He production limit.

Author contributions All authors contributed to the study conception and design. Material preparation, data collection, and analysis were performed by HMŞ, GT, AK, and MMO. The first draft of the manuscript was written by HMŞ, and all authors commented on previous versions of the manuscript. All authors read and approved the final manuscript.

References

1. L.A. El-Guebaly, Fifty years of magnetic fusion research (1958–2008): Brief historical overview and discussion of future trends. Energies **3**, 1067–1086 (2010). https://doi.org/10.3390/en30601067
2. ITER, EDA, Documentation Series No. 24 ITER Technical Basis. IAEA, Vienna -pub. iaea.org/MTCD/publications/PDF/ITER-EDA-DS-24. pdf (2002).
3. M.E. Sawan, M.A. Abdou, Physics and technology conditions for attaining tritium self-sufficiency for the DT fuel cycle. Fusion Eng. Des. **81**, 1131–1144 (2006). https://doi.org/10.1016/j.fusengdes.2005.07.035
4. H.M. Şahin, Monte Carlo calculation of radiation damage in first wall of an experimental hybrid reactor. Ann. Nucl. Energy **34**, 861–870 (2007). https://doi.org/10.1016/j.anucene.2007.04.011
5. B. Soltani, M. Habibi, Tritium breeding ratio calculation for ITER tokamak using developed helium cooled pebble bed blanket (HCPB). J. Fusion Energy **34**, 604–607 (2015). https://doi.org/10.1007/s10894-015-9847-1
6. F.A. Hernández, P. Pereslavtsev, First principles review of options for tritium breeder and neutron multiplier materials for breeding blankets in fusion reactors. Fusion Eng. Des. **137**, 243–256 (2018). https://doi.org/10.1016/j.fusengdes.2018.09.014
7. K. Tobita, S. Nishio, A. Saito et al., Water-cooled solid breeding blanket for DEMO. Paper Presented at the 18th International Toki Conference (ITC18), February, Development of Physics and Technology of Stellarators/Heliotrons en route to DEMO, (Toki, Japan 2009)
8. S. Şahin, A. Şahinaslan, M. Kaya, Neutronic calculations for a magnetic fusion energy reactor with liquid protection for the first wall. Fusion Technol. **34**, 95–108 (1998). https://doi.org/10.13182/FST98-A56

9. S. Yalçin, M. Übeyli, A. Acir, Neutronic analysis of a high-power density hybrid reactor using innovative coolants. Sadhana **30**, 585–600 (2005). https://doi.org/10.1007/BF02703281
10. S. Şahin, H.M. Şahin, A. Acır, LIFE hybrid reactor as reactor grade plutonium burner. Energy Convers. Manag. **63**, 44–50 (2012). https://doi.org/10.1016/j.enconman.2011.12.031
11. M. Sawan, Tritium Breeding Potential of Lithium-Tin. APEX Proj. Meet. (1998).
12. M.Z. Youssef, M.E. Sawan, D.K. Sze, The breeding potential of "Flinabe" and comparison to "Flibe" in "CliFF" high power density concept. Fusion Eng. Des. **61**, 497–503 (2002). https://doi.org/10.1016/S0920-3796(02)00245-4
13. H.M. Şahin, G. Tunç, N. Şahin, Investigation of tritium breeding ratio using different coolant material in a fusion-fission hybrid reactor. Int. J. Hydrogen Energy **41**, 7069–7075 (2016). https://doi.org/10.1016/j.ijhydene.2015.11.174
14. H.M. Şahin, A. Acır, T. Altınok et al., Monte Carlo calculation for various enrichment lithium coolant using different data libraries in a hybrid reactor. Energy Convers. Manag. **49**, 1960–1965 (2008). https://doi.org/10.1016/j.enconman.2007.09.028
15. M. Übeyli, On the tritium breeding capability of Flibe, Flinabe, and Li $_{20}Sn_{80}$ in a fusion-fission (hybrid) reactor. J. Fusion Energy **22**, 51–57 (2003). https://doi.org/10.1023/B:JOFE.0000021555.70423.f1
16. S. Şahin, H.M. Şahin, H. Şahiner et al., Study on the fusion reactor performance with different materials and nuclear waste actinides. Int. J. Energy Res. **45**, 11759–11774 (2020). https://doi.org/10.1002/er.5708
17. J.P. Catalán, F. Ogando, J. Sanz et al., Neutronic analysis of a dual He/LiPb coolant breeding blanket for DEMO. Fusion Eng. Des. **86**, 2293–2296 (2011). https://doi.org/10.1016/j.fusengdes.2011.03.030
18. S. Wang, F.A. Hernández, E. Bubelis et al., Comparative analysis of the efficiency of a CO_2-cooled and a He-cooled pebble bed breeding blanket for the EU DEMO fusion reactor. Fusion Eng. Des. **138**, 32–40 (2019). https://doi.org/10.1016/j.fusengdes.2018.10.026
19. M.S. Tillack et al., Technology readiness of helium as a fusion power core coolant. Center Energy Res. **25**, 61 (2014)
20. R.R. Romatoski, L.W. Hu, Fluoride salt coolant properties for nuclear reactor applications: a review. Ann. Nucl. Energy **109**, 635–647 (2017). https://doi.org/10.1016/j.anucene.2017.05.036
21. R. Boullon, J.-C. Jaboulay, J. Aubert, Molten salt breeding blanket: Investigations and proposals of pre-conceptual design options for testing in DEMO. Fusion Eng. Des. **171**, 112707 (2021). https://doi.org/10.1016/j.fusengdes.2021.112707
22. L.C. Cadwallader, Qualitative reliability issues for in-vessel solid and liquid wall fusion designs. Fusion Technol. **39**, 991–995 (2001). https://doi.org/10.13182/fst01-a11963371
23. F. Dobran, Fusion energy conversion in magnetically confined plasma reactors. Prog. Nucl. Energy **60**, 89–116 (2012). https://doi.org/10.1016/j.pnucene.2012.05.008
24. G. Tunç, H.M. Şahin, S. Şahin, Evaluation of the radiation damage parameters of ODS steel alloys in the first wall of deuterium-tritium fusion-fission (hybrid) reactors. Int. J. Energy Res. **42**, 198–206 (2018). https://doi.org/10.1002/er.3782
25. T. Muroga, Vanadium alloys for fusion blanket applications. Mater. Trans. **46**(3), 405–411 (2005). https://doi.org/10.2320/matertrans.46.405
26. Q. Huang, C. Li, Y. Li et al., Progress in development of China Low Activation Martensitic steel for fusion application. J. Nucl. Materials **367**, 142–146 (2007). https://doi.org/10.1016/j.jnucmat.2007.03.153
27. G. McCracken, P. Stott, Chapter 13 - Fusion Power Plants, ed. by Garry McCracken, Peter Stott, Fusion (Second Edition), (Academic Press, 2013) 165–187 (2013). doi: https://doi.org/10.1016/B978-0-12-384656-3.00013-1
28. K. Ioki, G. Johnson, K. Shimizu et al., Design of the ITER vacuum vessel. Fusion Eng. Des. **27**, 39–51 (1995). https://doi.org/10.1016/0920-3796(95)90116-7
29. A. Araujo, C. Pereira, M.A.F. Veloso et al., Flux and dose rate evaluation of ITER system using MCNP-a preliminary simulation. Braz. J. Phys. **40**, 55053633 (2010). https://doi.org/10.1590/S0103-97332010000100010
30. X-5 Monte Carlo Team, "MCNP - Version 5, Vol. I: Overview and Theory", LA-UR-03–1987 (2003).
31. D. Garber, C. Dunford, S. Pearlstein, Data Formats and procedures for the evaluated nuclear data file, ENDF. No. BNL-NCS-50496; ENDF-102. Brookhaven National Lab., Upton, NY, USA, (1975).
32. M.E. Battat, ANS-6.1. 1 Working group, "American National Standard Neutron and Gamma-Ray Flux-to-Dose Rate factors". ANSI/ANS-6.1. 1–1977, American Nuclear Society, LaGrange Park, Illinois, USA, (1977).
33. R. Kinsey, Data formats and procedures for the evaluated nuclear data file, ENDF. No. BNL-NCS–50496 (ED. 2). Brookhaven National Lab. (1979).
34. P.F. Rose, ENDF-201: ENDF/B-VI summary documentation. No. BNL-NCS-17541; ENDF-201. Brookhaven National Lab., Upton, NY (United States), (1991).
35. T.A. Al-Kusayer, S. Şahin, A. Drira. CLAW-IV coupled 30 neutrons, 12 gamma-ray group cross sections with retrieval programs for radiation transport calculations. Radiation Shielding Information Center, RSIC Newsletter, Oak Ridge National Laboratory 4 (1988).
36. G. Tunc, Ph.D. Dissertation (Department of Energy Systems Engineering Gazi University, 2017) (in Turkish)
37. S. Şahin, H.M., Şahin, T. Tunç, Monte Carlo analysis of LWR spent fuel transmutation in a fusion-fission hybrid reactor system. Nucl. Eng. Technol. **50**, 1339–1348 (2018). https://doi.org/10.1016/j.net.2018.08.006
38. M., Rubel, Fusion neutrons: Tritium breeding and impact on wall materials and components of diagnostic systems. J. Fusion Energy **38**, 315–329 (2019). https://doi.org/10.1007/s10894-018-0182-1
39. Nuclear Data Center at Korea Atomic Energy Research Institute (KAERI). Nuclear Data Plotter, https://atom.kaeri.re.kr/nuchart/plotEvaf.jsp; [accessed October 19, 2021].
40. R.W. Moir, R.L. Bieri, X.W. Chen et al., HYLIFE-II: a molten-salt inertial fusion energy power plant designing. Final Report. Fusion Technol. **25**, 5–25 (1994). https://doi.org/10.13182/FST94-A30234
41. D.L. Smith, C.C. Baker, D.K. Sze et al., Overview of the blanket comparison and selection study. Fusion Technol. **8**, 10–44 (1985). https://doi.org/10.13182/FST85-4
42. J.A. Blink, W.J. Hogam, J. Hovingh et al. High-yield lithium-injection fusion-energy (HYLIFE) reactor. No. UCRL-53559. Lawrence Livermore National Lab., CA, USA, (1985). doi: https://doi.org/10.2172/6124368
43. M. Perlado et al. Radiation Damage in Structural Materials, Energy from Inertial Fusion, International Atomic Energy Agency, 272, Vienna (1995).
44. M. Herman, A. Trkov, R. Capote et al., Evaluation of neutron reactions on iron isotopes for CIELO and ENDF/B-VIII. 0. Nuclear Data Sheets 148, 214–253 (2018). doi: https://doi.org/10.1016/j.nds.2018.02.004
45. J.J. Duderstadt, G.A. Moses, Inertial confinement fusion. (John Wiley & Sons, 1982).
46. E.A. Hofman, W.M. Stacey, N.E. Hertel et al., Radioactive waste disposal characteristics of candidate tokamak demonstration

reactors. Fusion Technol. **31**, 35–62 (1997). https://doi.org/10.13182/FST97-A30779

47. M.Z. Youssef, C. Wong, Neutronics performance of high temperature refractory alloy helium-cooled blankets for fusion application. Fusion Eng. Des. **49–50**, 727 (2000). https://doi.org/10.1016/S0920-3796(00)00182-4
48. A. S. T. M. Standard, Standard Practice for Characterizing Neutron Exposure in Iron and Low Alloy Steels in Terms of Displacements Per Atom (dpa). (2001).